Drug Delivery

ISSN: 1071-7544 (Print) 1521-0464 (Online) Journal homepage: https://www.tandfonline.com/loi/idrd20

Trans-nasal zolmitriptan novasomes: *in-vitro* preparation, optimization and *in-vivo* evaluation of brain targeting efficiency

Radwa M. A. Abd-Elal, Rehab N. Shamma, Hassan M. Rashed & Ehab R. Bendas

To cite this article: Radwa M. A. Abd-Elal, Rehab N. Shamma, Hassan M. Rashed & Ehab R. Bendas (2016) Trans-nasal zolmitriptan novasomes: *in-vitro* preparation, optimization and *in-vivo* evaluation of brain targeting efficiency, Drug Delivery, 23:9, 3374-3386, DOI: 10.1080/10717544.2016.1183721

To link to this article: https://doi.org/10.1080/10717544.2016.1183721

Accepted author version posted online: 29 Apr 2016.
Published online: 17 May 2016.

Drug Delivery

http://informahealthcare.com/drd
ISSN: 1071-7544 (print), 1521-0464 (electronic)

Drug Deliv, 2016; 23(9): 3374–3386
 DOI: 10.1080/10717544.2016.1183721

Taylor & Francis
Taylor & Francis Group

RESEARCH ARTICLE

Trans-nasal zolmitriptan novasomes: *in-vitro* preparation, optimization and *in-vivo* evaluation of brain targeting efficiency

Radwa M. A. Abd-Elal[1], Rehab N. Shamma[2], Hassan M. Rashed[3], and Ehab R. Bendas[4]

[1]*Department of Pharmaceutics and Industrial Pharmacy, Modern University for Technology & Information (MTI), Cairo, Egypt,* [2]*Department of Pharmaceutics and Industrial Pharmacy, Cairo University, Cairo, Egypt,* [3]*Labeled Compounds Department, Hot Laboratories Center, Egyptian Atomic Energy Authority, Cairo, Egypt, and* [4]*Clinical Pharmacy Department, Future University in Egypt, New Cairo, Egypt*

Abstract

Migraine attack is a troublesome physiological condition associated with throbbing, intense headache, in one half of the head. Zolmitriptan is a potent second-generation triptan, prescribed for patients with migraine attacks, with or without an aura, and cluster headaches. The absolute bioavailability of zolmitriptan is about 40% for oral administration; due to hepatic first metabolism. Nasal administration would circumvent the pre-systemic metabolism thus increasing the bioavailability of zolmitriptan. In addition, due to the presence of microvilli and high vasculature, the absorption is expected to be faster compared to oral route. However, the bioavailability of nasal administered drugs is particularly restricted by poor membrane penetration. Thus, the aim of this work is to explore the potential of novel nanovesicular fatty acid enriched structures (novasomes) for effective and enhanced nasal delivery of zolmitriptan and investigate their nose to brain targeting potential. Novasomes were prepared using nonionic surfactant, cholesterol in addition to a free fatty acid. A 2^3 full factorial design was adopted to study the influence of the type of surfactant, type of free fatty acid and ratio between the free fatty acid and the surfactant on novasomes properties. The particle size, entrapment efficiency, polydispersity index, zeta potential and % zolmitriptan released after 2 h were selected as dependent variables. Novasomes were further optimized using Design Expert® software (version 7; Stat-Ease Inc., Minneapolis, MN), and an optimized formulation composed of Span® 80:Cholesterol:stearic acid (in the ratio 1:1:1) was selected. This formulation showed zolmitriptan entrapment of 92.94%, particle size of 149.9 nm, zeta potential of −55.57 mV, and released 48.43% zolmitriptan after 2 h. The optimized formulation was further examined using transmission electron microscope, which revealed non-aggregating multi-lamellar nanovesicles with narrow size distribution. DSC, XRD examination of the optimized formulation confirmed that the drug have been homogeneously dispersed throughout the novasomes in an amorphous state. *In-vivo* bio-distribution studies of ^{99m}Tc radio-labeled intranasal zolmitriptan loaded novasomes were done on mice, the pharmacokinetic parameters were compared with those following administration of intravenous ^{99m}Tc-zolmitriptan solution. Results revealed the great enhancement in zolmitriptan targeting to the brain, with drug targeting potential of about 99% following intranasal administration of novasomes compared with the intravenous drug solution. Zolmitriptan loaded novasomes administered via the nasal route may therefore constitute an advance in the management of acute migraine attacks.

Keywords

Brain targeting, factorial design, intranasal route, novasomes, pharmacokinetics, radio-labeling, zolmitriptan

History

Received 14 March 2016
Revised 19 April 2016
Accepted 25 April 2016

Introduction

Zolmitriptan (ZT), 4S-4-((3-(2-(dimethylamino) ethyl)-1H-indol-5-yl) methyl)-1, 3-oxazolidin-2-one, is a potent second-generation triptan prescribed for patients with migraine attacks, with or without an aura, and cluster headaches. It has a very effective in reducing migraine symptoms, including pain, nausea and photo- or phonophobia (Glen et al., 1995). ZT mimics the action of serotonin by directly stimulating the serotonin receptors in the brain and thus leads to vasoconstriction of the blood vessels of the brain. Reduction in inflammation associated with antidromic neuronal transmission by ZT is yet another mechanism by which it has been reported to provide relief of acute migraine attacks (Rolan & Martin, 1998). ZT has been proven to inhibit the activation of trigeminovascular system, thereby reducing the neurogenic inflammation, constricting the dilated meningeal vessels and restraining the release of vasoactive neuropeptides (Pascual, 1998). ZT belongs to BCS class III, with high solubility and low permeability. The absolute bioavailability of ZT is about 40–50% for both oral and nasal dosage forms (Alhalaweh et al., 2009). The peak-plasma

Address for correspondence: Rehab Nabil Shamma, Department of Pharmaceutics, Faculty of Pharmacy, Cairo University, Kasr El-Aini Street, Cairo, Egypt. Tel: +20124099394, +20233456006. Email: rehab.shamma@pharma.cu.edu.eg, rehab_shamma@hotmail.com

concentration is achieved in about 1.5–3.5 h depending on the formulation, and the elimination half-life is 2.5–3 h. Oral ZT tablets possess several drawbacks, such as slow onset of action (Dowson & Charlesworth, 2002), low bioavailability and large inter-subject variability in the rate of absorption. Patients with migraine generally suffer from nausea and vomiting, therefore oral treatment can be inconvenient or could fail. In addition, migraine attacks delay gastric emptying resulting into delayed absorption during attacks. Therefore, nasal delivery could provide fast-acting, noninvasive treatment for migraine attacks. However, nasal administration of ZT poses a great challenge due to its low-membrane permeability. It was reported that ZT has low permeability, prolonged absorption down the gastrointestinal tract (Dixon & Warrander, 1997; Prajapati et al., 2014).

Scientific and technological advancements have been focused on increasing bioavailability and efficiency of ZT, such as orally disintegrating tablets, and sublingual tablets (Mahmoud & Salah, 2012; Prajapati et al., 2014; El-Setouhy et al., 2015). Direct transport of drugs to the brain circumventing the brain-barriers following intranasal administration provides a unique feature and better option to target drugs to the brain. Intranasal administration of ZT for direct transport to the brain via microemulsion (Vyas et al., 2005), polymeric microparticles (Gavini et al., 2013), nanoparticles (Girotra et al., 2016), and micellar nanocarriers (Jain et al., 2010) have been developed. ZT nasal spray was approved by the FDA in 2003. However, this simple aqueous solution succeeded to reach only same bioavailability of the oral tablet, which is already impaired by the first pass metabolism. Therefore, there is a growing need for the development of effective nasal dosage forms in order to deliver the drug to the brain and produce therapeutic effects.

Nonionic surfactant vesicles have been widely studied as an alternative to liposomes in order to overcome the problems associated with stability, sterilization and large-scale production (Azmin et al., 1985; Abdelkader et al., 2014). Niosomes are essentially nonionic surfactant based uni-lamellar or multi-lamellar vesicles in which an aqueous solution is entirely enclosed by a membrane resulting from the organization of surfactant molecules as bilayers. They can entrap hydrophilic drugs in compartments or lipophilic drugs by partitioning of these molecules into bilayer domains.

Novasome technology is a patented encapsulation process, initially developed by Novavax, IGI laboratories for effective delivery of a variety of substances. Novasomes are the modified forms of liposomes or a variation of niosomes prepared from the mixture of monoester of polyoxyethylene fatty acids, cholesterol and free fatty acids (Anupama et al., 2011). Novasomes are found to have several characteristics; being a multi bilayered vesicle with a high capacity central core in specific size range, it can deliver a large volume of active ingredient. Various vaccines based on novasomes have been licensed (Gregoriadis, 1995; Chambers et al., 2004).

Being fatty acid enriched vesicles, novasomes are expected to have better permeation through the nasal membrane and enhance nose to brain targeting potential of the drug loaded. Therefore, the aim of this work is to explore the potential of novasomes for effective and enhanced nasal delivery of ZT. The effects of formulation variables on the entrapment efficiency, particle size and zeta potential as well as the drug release was evaluated using full factorial design. Furthermore, ZT was radio-labeled using ^{99m}Tc in order to study ZT bio-distribution and pharmacokinetics after nasal administration of the developed ^{99m}Tc-ZT loaded novasomes to male albino mice and compared to intravenous ^{99m}Tc-ZT solution.

Materials and methods

Materials

ZT was kindly provided by Global Nabi Pharmaceutical Co. (Cairo, Egypt). Cholesterol®, Tween® 20, 40, 60, 80 and 85, Fluka Biochemical Co., Sigma Aldrich, Germany. Span® 60, 80 and 85, were purchased from, Merck, Schuchardit OHG, Germany. Span® 20, Atlas chemical industries, Wilmington, DE. Oleic acid, Stearic acid, disodium hydrogen phosphate, potassium di-hydrogen phosphate, potassium chloride and sodium chloride, were purchased from El-Nasr Chemical Co. (Cairo, Egypt). Methyl alcohol absolute (99%), United Company for chemical and medical preparations (Cairo, Egypt). Chloroform, Labscan Ltd, Dublin, Ireland. Dialysis tubing cellulose membrane (molecular weight cut off 12,000–14,000) was purchased from Sigma Aldrich, Germany. Technetium-99m was eluted as $^{99m}TcO_4^-$ from ^{99}Mo/^{99m}Tc generator, Monrol Company, Kocaeli, Turkey. All other chemicals and solvents were of analytical grade and were received without any further modifications.

Preparation of ZT-loaded niosomes and novasomes

ZT-loaded niosomes were prepared using the thin film hydration technique. Cholesterol and different ratio of the surfactant together with 20 mg ZT, were dissolved in 10 mL chloroform, and added to a 250 mL round bottom flask. The organic solvent was slowly evaporated under reduced pressure, using a Rotavapor, Type R 110 (Büchi, Switzerland) under vacuum at 60 °C till a dry thin film was obtained on the walls of the round bottom flask. The produced film was hydrated with 10 mL phosphate buffer saline pH = 7.4 for 1 h at 60 °C with continuous stirring with the aid of small glass beads (eight small glass beads, each of diameter of 4 mm) to facilitate the hydration of the thin film. The prepared nano-dispersion was refrigerated overnight at (4 °C) for maturation. As for the novasomes, the free fatty acid was first dissolved in the chloroform, together with the surfactant, cholesterol and the drug was then processed using the same procedure mentioned above.

Evaluation of the ZT-loaded niosomes and novasomes

Determination of % ZT entrapment efficiency (E.E %)

One milliliter of freshly prepared nano-dispersion was separated from the un-entrapped drug using cooling ultracentrifuge (Model 8880, Centurion Scientific Ltd., W. Sussex, UK) at 4 °C and speed of 15000 rpm for 1 h. The supernatant (un-entrapped drug) was separated from the residue then the residue was washed with distilled water to ensure complete removal of the un-entrapped drug from the voids between the vesicles (Mokhtar et al., 2008), re-centrifuged at 4 °C and

15000 rpm for 1 h. The supernatant was discarded, and suitable amount of methanol was added to the residue. The mixture was shaken well to dissolve the vesicles in order to release the entrapped ZT (Tavano et al., 2013), then measured spectrophotometrically after appropriate dilution (Shimadzu UV-1601 Double Beam Spectrophotometer, Kyoto, Japan) at λ_{max} 285 nm using methanol as a blank. Each experiment was carried out in triplicate.

The E.E (%) was calculated using the following equation (1) (Bendas et al., 2013).

$$\text{E.E } (\%) = \frac{ED}{TD} \times 100 \quad (1)$$

Where: ED: is the concentration of entrapped drug.
TD: is the total drug concentration.

Particle size analysis and polydispersity index (PDI)

The particle size and PDI were determined by the photon correlation spectroscopy using a Malvern Zetasizer Nano (Malvern Instruments, Malvern, Worcestershire, UK) at an angle of 90 °C in 10 mm diameter cells at 25 °C (Basha et al., 2013). Before particle size measurement, one milliliter from each formulation was appropriately diluted with 15 mL distilled water to have a suitable scattering intensity. Results were obtained as mean values ($n = 3 \pm$ SD).

Zeta potential (ZP) analysis

ZP was determined by photon correlation spectroscopy using a Malvern Zetasizer Nano at an angle of 90° in 10 mm diameter cells at 25 °c. Before ZP measurements, the formulations were diluted appropriately with 15 mL distilled water and the ZP of the ZT-loaded novasomes vesicles was determined by observing their electrophoretic mobility in an electrical field (Basha et al., 2013). Results were obtained as mean values ($n = 3 \pm$ SD).

In-vitro *release studies of ZT-loaded novasomes*

The USP Dissolution test apparatus (Pharma Test dissolution Tester, Germany) was used to study the drug release from different ZT-loaded novasomes and ZT aqueous solution. The dialysis method was applied using cellulose membrane, where a constant volume of ZT-loaded novasomes (equivalent to 2 mg ZT) were placed in a glass cylinder (2.5 cm in diameter and 7.5 cm in length). Each tube was tightly covered with a cellulose membrane presoaked in PBS (pH = 7.4) from one end and attached to the shaft instead of baskets, from the other end. The shafts were then lowered to beakers containing 50 mL of PBS (pH = 7.4) as a dissolution medium till surface of cylinder touch the surface of the dissolution medium (Tavano et al., 2013). These beakers were water jacketed inside the vessels of the dissolution apparatus to keep a constant temperature during the experiment. The cylinders were adjusted to rotate at a constant speed (100 rpm) at 37 °C. The vessels were covered during experiment to minimize evaporation of dissolution medium. Samples of 3 mL were withdrawn periodically at predetermined time intervals (0.5, 1, 2, 3, 4, 5, 6, 7,8, 24 h)and replaced with fresh medium to maintain sink conditions, and measured spectrophotometrically at λ_{max} 283 nm using PBS (pH = 7.4) as a blank. Results were taken as mean values ($n = 3 \pm$ SD).

Statistical design of the study

A 2^3 full factorial design was employed to statistically investigate the effect of different formulation variables on the properties of ZT-loaded novasomes. The responses of all model formulations were treated by Design-Expert® software (version 7; Stat-Ease, Inc., Minneapolis, MN). The type of surfactant (SAA) (X_1), type of free fatty acid (FFA) (X_2) and ratio of free fatty acid to surfactant (FFA:SAA) (X_3) were selected as the independent variables. The E.E (%) (Y_1), particle size (Y_2), PDI (Y_3), ZP (Y_4) and ZT release after 2 h (%) (Y_5) were selected as the dependent variables. The design parameters and experimental runs are shown in Tables 1 and 2, respectively. Desirability was calculated for selection of the optimized formula which was subjected for further investigations.

Transmission electron microscopy (TEM)

The morphologic examination of the optimized formulation was performed by a TEM (JEOL JEM1230, Tokyo, Japan) operating at an accelerating voltage of 80 kV. One drop of dispersion was deposited on the surface of a carbon-coated copper grid and left to adhere on the carbon substrate for 1 min and any excess of dispersion was removed by a tip of filter paper (Tavano et al., 2013; Shamma & Aburahma, 2014).

Thermal analysis of ZT-loaded novasomes

Differential scanning calorimetry (DSC)

The optimized ZT-loaded novasomes formula was lyophilized (Novalyphe-NL 500; Savant Instruments Corp., Hicksville, NY, USA) in order to transfer it into dry powder before DSC analysis. ZT, Span® 80, stearic acid, cholesterol and lyophilized ZT loaded novasomes were subjected to DSC (PerkinElmer, Waltham, MA). Approximately 4 mg of samples were analyzed in sealed aluminum pans in the temperature range from 30 to 300 °C at a heating rate of 10 °C/min under inert nitrogen flow (25 mL/min) (Shamma & Aburahma, 2014).

X-ray diffraction (XRD)

Similar to DSC analysis, the optimized ZT-loaded novasomes formula was lyophilized. The XRD analysis (Scintag Inc.,

Table 1. Design parameters and constraints for full factorial design (2^3).

Independent variables	Level of variables
X_1: Type of SAA	Span® 60 (S 60) Span® 80 (S 80)
X_2: Type of FFA	Oleic Acid Stearic Acid
X_3: Ratio of FFA: SAA	1:1 2:1
Responses	Constraints
Y_1: E.E (%)	Maximize
Y_2: Particle size (nm)	Minimize
Y_3: PDI	Minimize
Y_4: ZP (mV)	Maximize
Y_5: ZT release after 2 h (%)	Maximize

Santa Clara, CA) of ZT, stearic acid, cholesterol and lyophilized ZT-loaded novasomes of the optimized formulation were conducted by powder XRD. (Shamma & Aburahma, 2014).

In-vivo bio-distribution and pharmacokinetics studies

Radio-labeling of ZT

ZT was radiolabeled by Tc-99m using direct labeling method (Babbar et al., 2000). Sodium dithionite was used as the reducing agent in order to avoid colloidal stannic oxide interference with bio-distribution pattern in case of using $SnCl_2$ as the reducing agent (Qi et al., 1996; Geskovski et al., 2013). The formulation was prepared using the radiolabeled drug. The effect of ZT amount, sodium dithionite amount, incubation time, pH and reaction temperature on radiolabeling efficiency were studied to achieve optimum reaction conditions. The radiochemical yield of ^{99m}Tc-ZT was estimated using ascending paper chromatography and thin layer chromatography. A dual solvent systems consisting of acetone and ethanol:water:ammonium hydroxide mixture (2:5:1, v/v/v) were used as mobile phases (Essa et al., 2015). The optimized radiolabeled-drug complex was assessed for *in-vitro* stability.

Bio-distribution studies

The drug bio-distribution and pharmacokinetic studies were conducted in accordance with the guidelines set by the Egyptian Atomic Energy Authority for animal experiments. The protocol of the study was reviewed and approved by the institutional review board; Research Ethics Committee Faculty of Pharmacy, Cairo University (REC-FOPCU) in Egypt. The studies were carried out in male Swiss albino mice (20–25 g). The animals were housed under constant environmental (room temperature 25 ± 0.5 °C relative humidity; 65% with a 12 h on/off light schedule) and nutritional conditions (fed with standard mice diet with free access to water) throughout the experimental period. On the study day, the mice were divided into 2 groups (21 mice per group). The conscious animals were administered intravenous (I.V.) ^{99m}Tc-ZT aqueous solution (group A), intranasal (I.N.) ^{99m}Tc-ZT-loaded novasomes (group B) at a ZT dose equivalent to 0.02 mg/g body weight. Briefly, 80–100 µL ^{99m}Tc-ZT solution (containing about 0.02 mg of ZT) was injected through the tail vein of the mice. In a parallel line, 20–25 µL of ^{99m}Tc-ZT-loaded novasomes containing an equivalent amount of ZT were instilled into each nostril using a micropipette (200 µl) fixed with low-density polyethylene tube having 0.1 mm internal diameter at the delivery site. During the I.N. administration, the mice were held from the back in a slanted position. The formulations were administered at the openings of the nostrils. The procedure was performed gently, allowing the animals to inhale all the preparation. At different time intervals (0.25, 0.5, 1, 2, 4, 6 and 24 h), three mice were anesthetized by chloroform. The blood samples were collected by cardiac puncture. Subsequently, the brain was dissected, washed with normal saline, made free from adhering tissue/fluid, and weighed. The weight of the individual tissue/organ was determined. The radioactivity of each sample as well as the background was counted in a well-type NaI (Tl) crystal coupled to SR-7 scaler ratemeter (Motaleb et al., 2011, 2012; Rashed et al., 2014). Percent injected dose per gram (%ID/g ± S.D.) in a population of three mice for each time point are reported. Data were evaluated using one way ANOVA test. Results for p-values are reported and all the results are given as mean ± SEM. The level of significance was set at $p < 0.05$.

The pharmacokinetics parameters of both formulations were calculated by WinNonlin® software program (Ver. 1.5, scientific consulting Inc., Cary, NC) by non-compartment analysis (Abdelbary & Tadros, 2013). The mean ZT radioactivity uptake (%ID/g) in blood and brain samples were plotted against time (h) and the maximum concentration of ZT uptake (C_{max}) and the time to reach it (T_{max}) were easily recorded. The area under the curve from 0 to 24 h ($AUC_{(0–24)}$, h. %ID/g), the area under the curve from 0 to infinity ($AUC_{(0-\infty)}$, h. %ID/g), the time to reach half plasma concentration ($t_{1/2}$, h) and the mean residence time (MRT, h) were also estimated.

The evaluation of the ZT brain targeting after I.N. application was estimated by using drug to brain direct transport percentage (DTP %) (Zhang et al., 2004; Vyas et al., 2005) (equations 2–3).

$$\text{DTP } (\%) = \frac{(BI \cdot N - Bx)}{BI \cdot N} \times 100 \qquad (2)$$

Table 2. Experimental runs independent variables (formulation variables) of the 2^3 full factorial experimental design.

	Factors (Independent variables)			Dependent variables				
Run	X_1: Type of SAA	X_2: Type of FFA	X_3:Ratio of FFA:SAA	Y_1:E.E (%)	Y_2: Particle size (nm)	Y_3:PDI	Y_4:ZP (mV)	Y_5: ZT release after 2h (%)
R1	S 60	Oleic acid	1:1	98.31 ± 1.75	656.56 ± 79.32	0.468 ± 0.14	−63.77 ± 1.12	46.29 ± 0.92
R2	S 60	Oleic acid	2:1	48.05 ± 5.50	368.60 ± 77.98	0.540 ± 0.11	−68.10 ± 10.18	38.05 ± 1.24
R3	S 60	Stearic acid	1:1	99.30 ± 0.65	494.96 ± 89.10	0.895 ± 0.09	−64.63 ± 5.39	45.08 ± 3.37
R4	S 60	Stearic acid	2:1	88.83 ± 1.16	482.36 ± 35.11	0.930 ± 0.09	−50.97 ± 1.97	55.71 ± 2.37
R5	S 80	Oleic acid	1:1	71.12 ± 3.09	201.03 ± 8.98	0.315 ± 0.04	−51.57 ± 2.20	38.88 ± 1.32
R6	S 80	Oleic acid	2:1	33.41 ± 1.75	242.00 ± 53.89	0.396 ± 0.04	−54.27 ± 1.97	29.81 ± 0.48
R7	S 80	Stearic acid	1:1	92.94 ± 1.04	149.90 ± 10.92	0.477 ± 0.10	−55.57 ± 1.04	48.43 ± 1.64
R8	S 80	Stearic acid	2:1	87.01 ± 1.66	199.90 ± 98.89	0.563 ± 0.00	−54.63 ± 2.65	55.75 ± 2.06

N.B.: Drug concentration was kept constant 2 mg/ml in all formulations.
Data are mean values ($n = 3$) ± S.D.

Where, $B_{I.N}$: is the total brain $AUC_{(0–24)}$ after I.N administration.

B_X: is AUC fraction contributed by systemic circulation through blood brain barrier (BBB) after I.N administration and it is determined according to equation (3).

$$B_x = \frac{BI.VXPI.N}{PI \cdot V} \quad (3)$$

Where, $B_{I.V}$: is the brain $AUC_{(0–24)}$ after I.V. administration.

$P_{I.V.}$ is the blood $AUC_{(0–24)}$ after I.V. administration.

$P_{I.N.}$ is the blood $AUC_{(0–24)}$ after I.N administration.

The data in the form of mean values (±SD) of three determinations were statistically analyzed applying one way ANOVA using SPSS 17 software (version 17, SPSS Inc., Chicago, IL). Post-hoc multiple comparisons were performed using Fisher's least significant difference test and the results were considered significantly different when p values were less than 0.05.

Results and discussion

Characterization of ZT-loaded niosomes

The E.E (%) is one of the important parameters in the design of vesicular formulations. Vesicular E.E relies on the stability of the vesicles which is highly dependent on the type of surfactant forming the bilayers. Therefore, the effects of these different parameters were evaluated and optimized. In our preliminary experiments, different nonionic surfactants were examined in the preparation of ZT loaded niosomes, namely: Span® 20, Span® 40, Span® 60, Span® 80, Tween® 20, Tween® 40, Tween® 60, Tween® 80, Tween® 85. From the results obtained, only Span® 60, and Span® 80 showed acceptable results regarding drug entrapment, and particle size (data not shown). The significant effect of lipophilic surfactant on E.E (%) of ZT-loaded niosomal dispersions encouraged us to study the effect of FFA, in order to prepare ZT-loaded novasomes dispersions with higher E.E (%) while keeping the size in the nano-range. Full factorial design (2^3) was used to study the effect of type of SAA, type of FFA and ratio of FFA: SAA on the properties of ZT-loaded novasomes dispersions.

Statistical analysis of the experimental design

Effect of formulation variables on the E.E (%)

In order to deliver a sufficient amount of drug, a high entrapment of the drug within the vesicular structure is required (Pavelic et al., 2001). Therefore, it is necessary to decrease the leakage of an entrapped drug (Kulkarni et al., 1995). Results show that the type of SAA (X_1) and type of FFA (X_2) have a significant impact on the E.E (%) of ZT-loaded novasomes ($p<0.0001$) (Figure 1a). Span® 60 containing vesicles have a significantly higher E.E (%) compared on those containing Span® 80. This could be attributed to the solid nature, hydrophobicity and phase transition temperature (T°c) of the Span® 60 (Toshimitsu et al., 1994). Span® 60 has higher T°c (53 °C) than Span® 80 (−12 °C) (Kibbe, 2000), thus provides higher entrapment for the drug (Toshimitsu et al., 1994).

Another reason is the degree of saturation of the alkyl chain length. Although both surfactants have the same alkyl chain length (C_{18}) (Devaraj et al., 2002), the oleate moiety of Span® 80 has a double bond (with relatively high electron density) at C_9, which repels the adjacent hydrocarbon chains resulting in the characteristic 'kink' in the structure (Toshimitsu et al., 1994; Abdelkader et al., 2014). This causes the membrane to be more permeable, and explains why Span® 80 containing novasomes had lower E.E (%) than those with Span® 60. This is in accordance with the results obtained by Al-Mahallawi et al, in their study on the preparation of tenoxicam loaded bilosomes (Al-Mahallawi et al., 2015). They found that the E.E (%) of Span® 60 containing vesicles had a significantly higher E.E than those containing Span® 80 and Span® 20 as a surfactant. They related that to the highest saturation of the alkyl chain length and (T°c) of Span® 60, which affected the drug E.E (%) in the prepared bilosomes (Al-Mahallawi et al., 2015).

Stearic acid containing vesicles had a significantly higher E.E (%), compared to those containing oleic acid as a FFA. This may be related to the degree of saturation of the alkyl chain of the FFA. Both stearic acid and oleic acid have the similar alkyl chain length (C_{18}). However, oleic acid has an un-saturated double bond in its alkyl chain, which affects its T°c. Oleic acid has lower T°c (13°C) than that of stearic acid (69°C), which forms more leaky vesicles, resulting in lower entrapment (Kanicky & Shah, 2002).

A significant interaction between the type of SAA (X_1), and the type of FFA (X_2) on the E.E (%) was observed ($p=0.007$) (Figure 1a). Span® 80 containing vesicles had a significantly a lower E.E (%) in presence of oleic acid than stearic acid. This may be related to the presence of un-saturation in the alkyl chain of both oleic acid and Span® 80, which has a synergistic effect on the formation of a more permeable and leaky vesicles. This results in ZT escape outside the vesicles and lowering the E.E (%).

A significant impact of the ratio of FFA: SAA (X_3) was also demonstrated ($p<0.0001$). Increasing the molar ratio of FFA from 1:1 to 2:1 resulted in a significant decrease in the E.E (%) of ZT-loaded novasomes (Figure 1b). This may be attributed to possible existence of mixed micelles in the dispersion medium, which increases the drug solubility in the dispersion medium with the increase in FFA concentration, thereby lowering the E.E (%).

Effect of formulation variables on the particle size and PDI

Statistical analysis using ANOVA showed that type of SAA (X_1) had a significant impact on the particle size of ZT-loaded novasomes ($p<0.0001$). Span® 60 containing vesicles had a significantly higher particle size compared on those containing Span® 80 (Figure 1c). According to the literature, increasing the HLB value of the surfactant monomers (decrease lipophilicity) leads to the formation of larger vesicles owing to the increase in surface free energy (Aggarwal et al., 2004; Abdelkader et al., 2010). Span® 60 has higher HLB (4.7) compared to Span® 80 (4.3) (Lingan et al., 2011). A correlation between the particle size of the vesicles and the drug E.E (%) was observed, where the larger particle size novasomes (containing Span® 60) had a higher

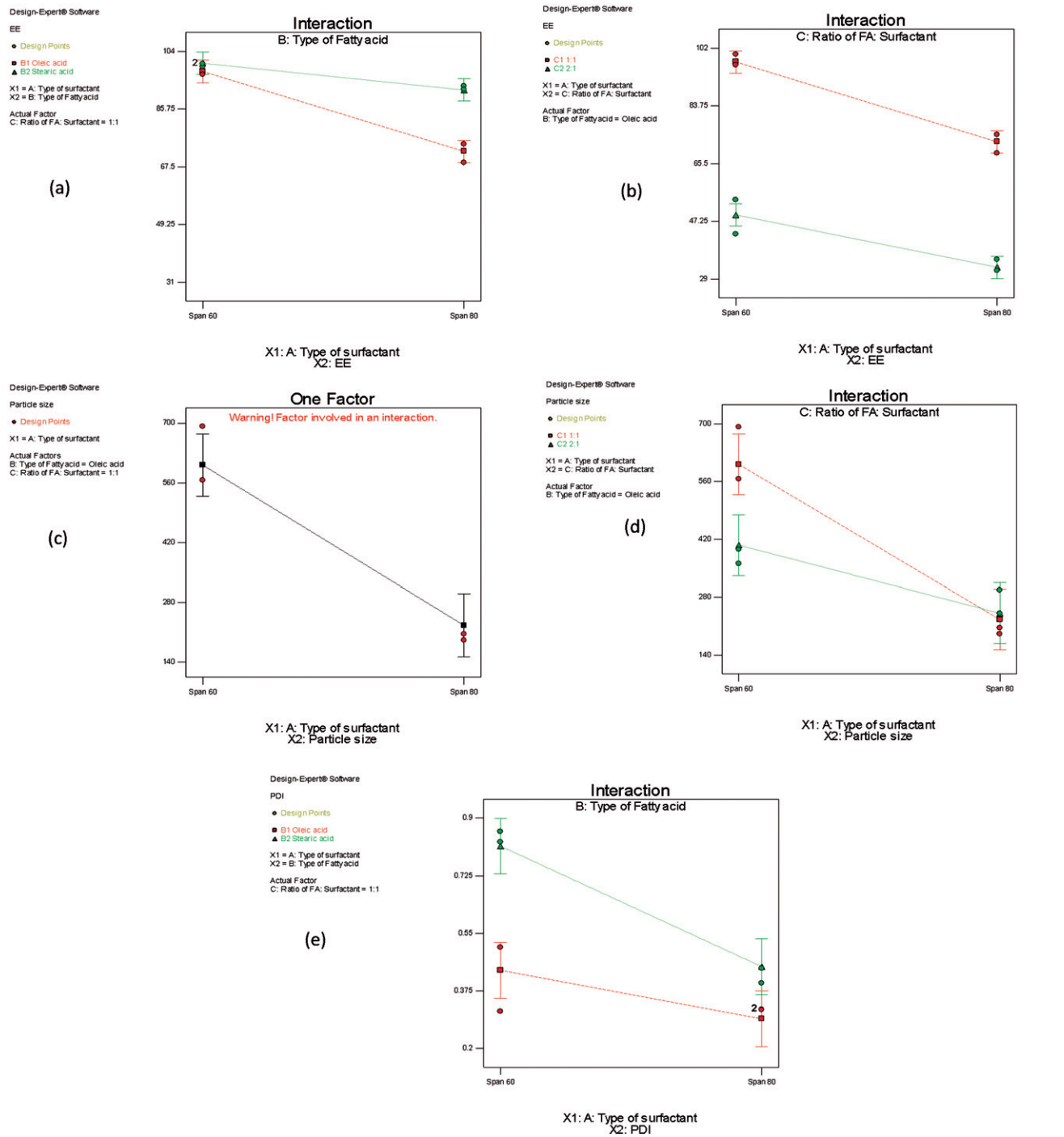

Figure 1. Line charts showing the effects of (a) type of SAA (X_1) and the FAA (X_2) on the E.E (%) of ZT-loaded novasomes, (b) type of SAA (X_1) and the FAA (X_3) on the E.E (%) of ZT-loaded novasomes, (c) type of SAA (X_1) on the particle size of ZT-loaded novasomes, (d) type of SAA (X_1) and the ratio of FAA: SAA (X_3) on the particle size of ZT-loaded novasomes, (e) type of SAA (X_1) and the type of FAA(X_2) on the PDI of ZT-loaded novasomes.

drug entrapment. This could be attributed to the increase in distance between the layers resulting in better drug inclusion in the hydrophobic area within the vesicles (El-Laithy et al., 2011). Similar results were observed by Al-Mahallawi et al, on preparing tenoxicam loaded bilosomes for transdermal delivery (Al-Mahallawi et al., 2015).

A significant interaction between type of SAA (X_1) and ratio of FFA: SAA (X_3) was observed ($p = 0.014$). The particle size of Span® 60 containing vesicles decreased significantly upon increasing the ratio of oleic acid: SAA from 1:1 to 2:1. However, only a slight decrease in the particle size of Span® 80 containing vesicles was observed upon increasing the ratio of oleic acid: SAA from 1:1 to 2:1 (Figure 1d).

The PDI was used as an indication for the width of particle size distribution, in order to indicate the uniformity of the vesicle size within the formulation. PDI is the ratio of standard deviation to mean droplet size (Centis & Vermette, 2008). A small value of PDI reveals a homogenous mono-disperse size distribution, while a large PDI value reflects a higher heterogeneous poly-disperse size distribution (Zeisig et al., 1996; Basha et al., 2013).

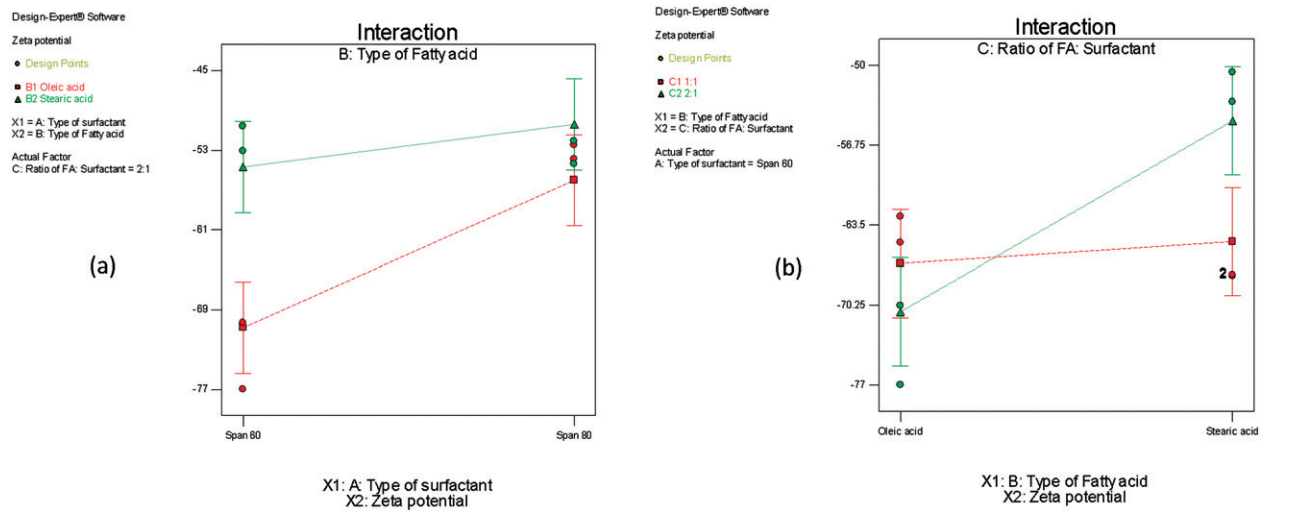

Figure 2. Line charts showing the effects of (a) type of SAA (X_1) and the FAA (X_2) on the ZP of ZT-loaded novasomes, (b) type of SAA (X_3) on the ZP of ZT-loaded novasomes.

Statistical analysis using ANOVA showed that type of SAA(X_1) had a significant impact on the PDI of ZT-loaded novasomes dispersions ($p = 0.0004$). Span® 80 containing vesicles showed significantly lower PDI and good homogeneity compared to Span® 60 containing vesicles. This could be attributed to their lower particle size compared to novasomes prepared using Span® 60 (Al-Mahallawi et al., 2015).

A significant impact of the type of FFA (X_2) on the PDI of the prepared novasomes was also demonstrated ($p = 0.0001$). Oleic acid containing vesicles had a significantly lower PDI compared to those containing stearic acid as FFA. This may be related to the lower particle size obtained by oleic acid containing vesicles (Figure 1e).

Effect of formulation variables the ZP

ZP is the measure of the overall charges acquired by vesicles. It represents indirect measurement to judge the stability of colloidal dispersions. In general, the system is considered stable when ZP value is greater than +30 mV (Abdelbary & AbouGhaly, 2015). This ensures that the vesicles have sufficient charges that would inhibit their aggregation, owing to the electric repulsion between the vesicles. In the present study, the surface-charge properties of the prepared novasomes dispersions were investigated and results showed negative charges on their surfaces with ZP values ranging from -51.57 ± 2.02 to -68.10 ± 10.18 mV. Since all the formulations in our study had negative ZP, variation in ZP will be discussed in terms of its absolute value to avoid confusion.

Results show that type of SAA (X_1) had a significant impact on ZP of ZT-loaded novasomes dispersions ($p = 0.0007$). Span® 60 containing vesicles were found to have significantly higher ZP values than Span® 80 containing vesicles. This could be attributed to the lipophilicity of surfactant forming vesicles. Decreasing the lipophilicity of the surfactant increases the ZP values, owing to the reduction in surface free energy of the surfactant. Span® 60 (HLB = 4.7) is less lipophilic than Span® 80 (HLB = 4.3), therefore it showed higher ZP values than Span® 80 (Lingan et al., 2011).

A significant interaction between the type of SAA (X_1), and type of FFA (X_2) ($p = 0.0383$) was demonstrated. Changing the FFA from oleic acid to stearic acid resulted in significantly lower ZP values of Span® 60 containing vesicles compared to Span® 80 containing novasomes (Figure 2a). Also increasing the ratio of oleic acid: SAA from 1:1 to 2:1 resulted in significantly higher ZP values ($p = 0.0092$). Similar results were obtained by Manca et al. in their study on the preparation of rifapmicin liposomes (Manca et al., 2012). In contrast, increase ratio of stearic acid from 1 to 2 resulted in decreasing ZP of novasomes (Figure 2b).

Effect of formulation variables on the % ZT released after 2 h from ZT-loaded novasomes dispersions

Figure 3 illustrates the release profiles of different ZT loaded novasomes as well as the drug solution. The % ZT released from the solution was very high, with about 97% ZT released in the first 4 h. On the other hand, the prepared ZT-loaded novasomes succeeded to retard the drug release compared with the drug solution. The release of ZT from all novasomes was biphasic, showing an initial relatively fast release phase followed by a slower phase. This may be attributed to the rapid portioning of the surface adsorbed ZT with hydrophilic nature into the release medium accounting for the burst effect observed (Pardakhty et al., 2007). This indicates that ZT-loaded novasomes are expected to show a rapid onset of action due to its initial fast release phase followed by sustained drug delivery due to its slower phase.

ANOVA test was performed to evaluate the level of significance of the tested factors on the % ZT released from different novasomes after 2 h as well as the interactions between factors. A significant impact of the type of SAA (X_1) on the % ZT released after 2 h was demonstrated ($p = 0.0331$). Span® 60 containing vesicles had a significantly higher % ZT released compared on those containing Span® 80 as a surfactant. This could be attributed to the less hydrophobic nature of Span® 60, compared to Span® 80, which facilitated the drug diffusion to the release medium.

A significant impact of the type of FFA (X_2) on the % ZT release after 2 h was also demonstrated ($p < 0.0001$). Stearic

acid containing vesicles had a significantly higher % ZT released after 2 h compared on those containing oleic acid as a FFA. This could be attributed to smaller particle size and higher E.E (%) of stearic acid containing vesicles as FFA. Smaller vesicles lead to faster drug release due to larger surface area exposed to the dissolution medium (Shaul Hameed Maraicar & Narayanan, 2014). Moreover, the higher E.E (%), the higher % ZT released from the vesicles by drug diffusion though the vesicular bilayers.

A significant interaction between the type of SAA (X_1) and the type of FFA (X_2) was also observed ($p = 0.0027$). The % ZT released after 2 h from Span® 80 containing vesicles decreased significantly upon changing type of FFA from stearic acid to oleic acid, whereas, the % ZT released of Span® 60 containing vesicles were not significantly affected, Figure 4a. This could be attributed to the synergistic effect of both Span® 80, and oleic acid on retarding the release of ZT from the vesicles, owing to their higher hydrophobic nature, compared to Span® 60, and stearic acid.

A significant interaction between type of FFA (X_2), and ratio of FFA: SAA (X_3) on the % ZT drug released after 2 h was demonstrated ($p < 0.0001$). The % ZT released after 2 h from vesicles containing oleic acid as a FFA decreased significantly upon increasing ratio of oleic acid:SAA from 1:1 to 2:1. This could be attributed to the formation of oleic acid micelles at the higher ratio, which is known for a more retarding effect on the drug release than vesicles (Mittal et al., 2013). On the other hand, the % ZT released from vesicles

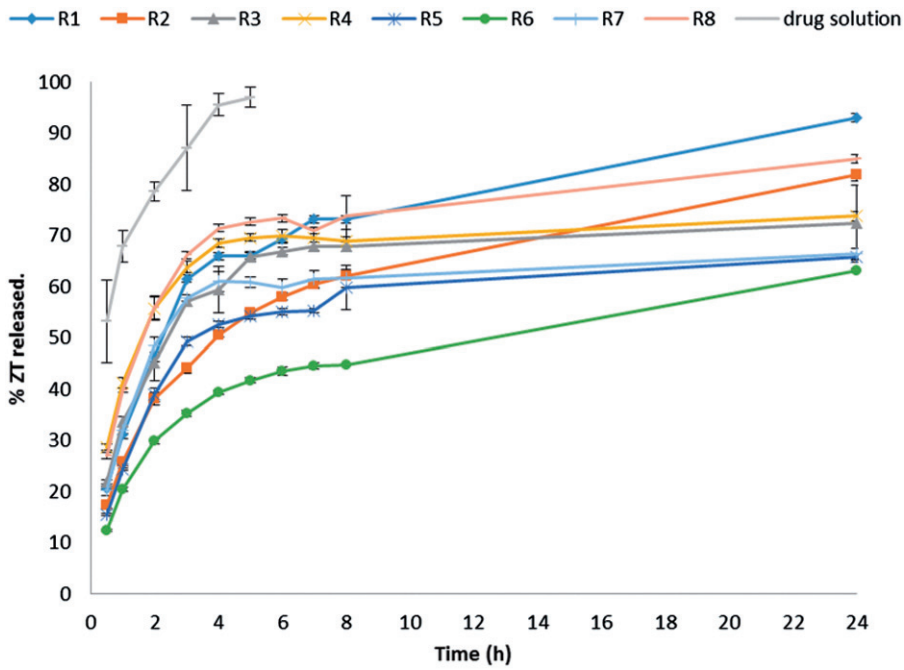

Figure 3. Release profiles of ZT from different ZT-loaded novasomes and ZT solution.

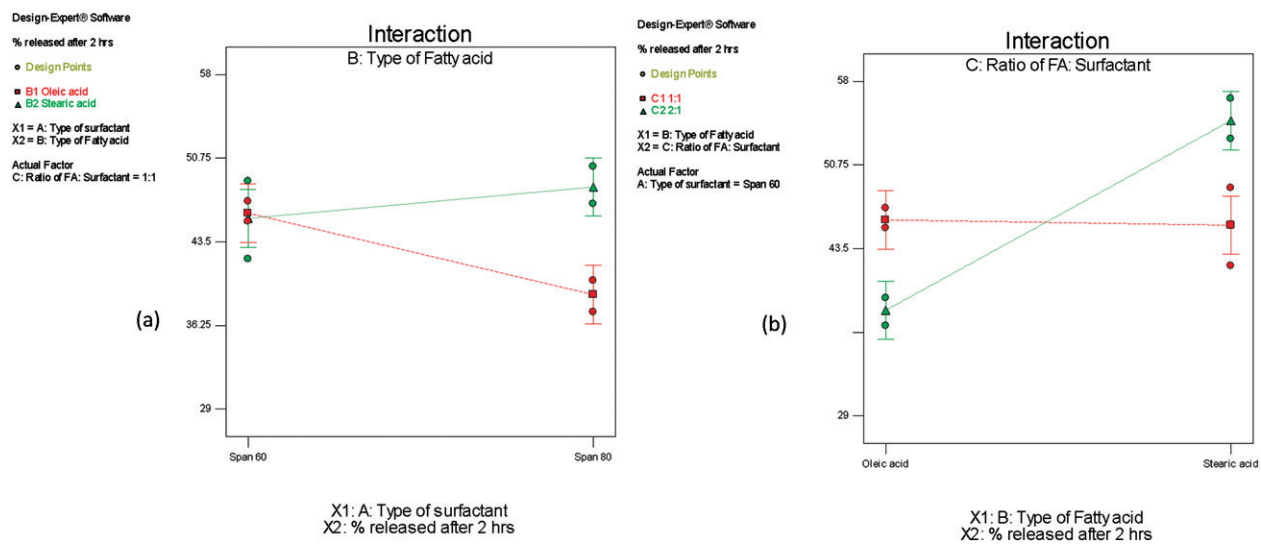

Figure 4. Line charts showing the effects of (a) type of SAA (X_1) and the FAA (X_2) on the ZT (%) released after 2h from ZT-loaded novasomes, (b) type of FAA (X_2) and the ratio of FAA: SAA (X_3) on the ZT (%) released after 2h from ZT-loaded novasomes.

containing stearic acid as a FFA was not significantly affected upon changing the ratio of stearic acid:SAA from 1:1 to 2:1 (Figure 4b).

Optimization

In order to find the level of each independent variable that will lead to select the optimized formulation, desirability was calculated by Design-Expert® software and considered to optimize the studied factors depending on the provided results from the prepared ZT-loaded novasomes. The optimization process was performed in order to obtain novasomes with maximum values of E.E (%), ZP, and % ZT release after 2 h, with minimum values for particle size and PDI by numerical analysis using the Design-Expert® software and based on the criterion of desirability (Basalious et al., 2010). The highest desirability value (0.794) was obtained by formulation (R7), composed of Span® 80: Cholesterol: stearic acid (in the ratio 1:1:1). This formulation showed E.E of (%) 92.94 ± 1.75, particle size of 149.9 ± 10.92 nm, PDI equal to 0.477 ± 0.10, ZP of -55.57 ± 1.04 mV, and released 48.43 ± 1.64% ZT released after 2 h. Hence, it was selected as the best performing formulation for further investigations. The optimized formulation was subjected to TEM, DSC, XRD and *in vivo* bio-distribution.

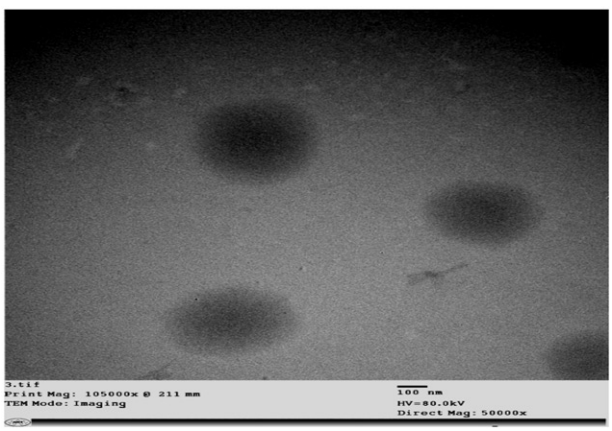

Figure 5. TEM image of optimized R7 dispersion.

TEM analysis

TEM analysis is a useful mean for examining the morphological characteristics of nanovesicles. The optimized formulation R7 was examined by TEM, and appeared to be non-aggregating multi-lamellar nanovesicles with a predominant spherical shape and narrow size distribution as shown in Figure 5. The figure clearly shows that the diameter of the vesicles observed in the micrograph was in the nano-range and in harmony with that measured by the Malvern particle size analyzer.

Thermal analysis of the optimized ZT-loaded novasomes

DSC analysis

DSC was used to investigate the crystalline or amorphous nature of the drug within the optimized formulation and to

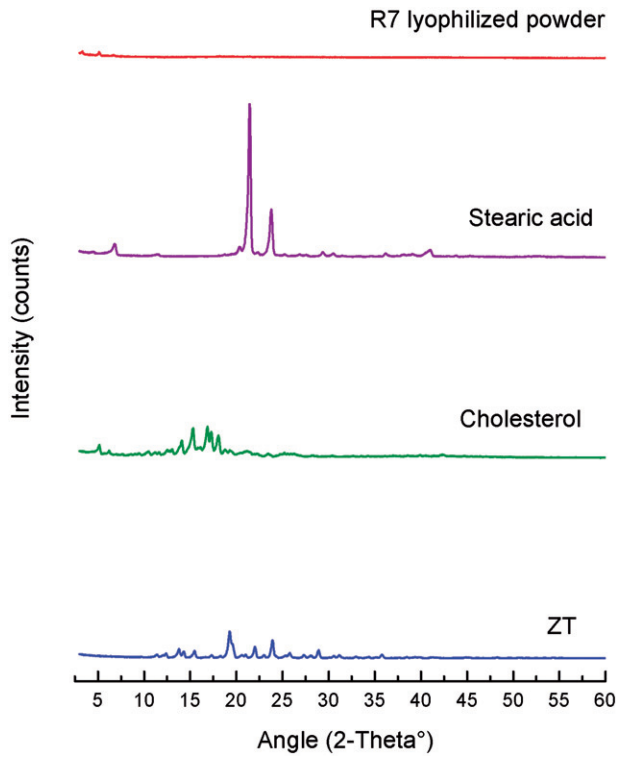

Figure 7. XRD spectra of the samples.

Figure 6. DSC thermographs of (a) stearic acid, (b) ZT, (c) cholestrol, (d) Span® 80 and (e) lyophilized (R7).

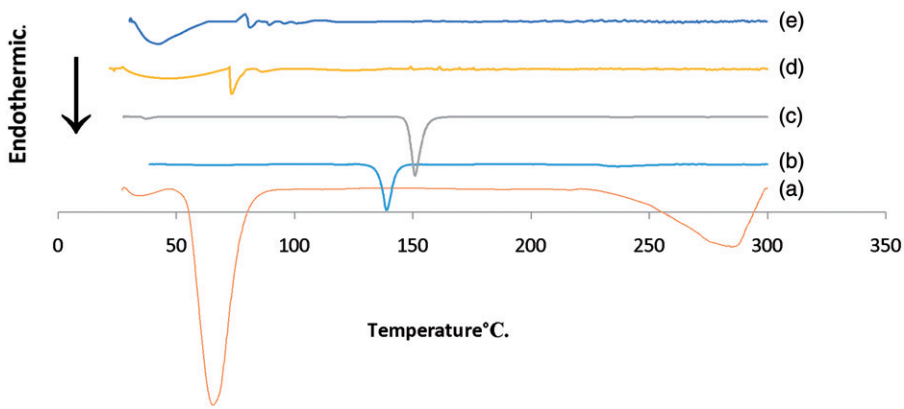

Table 3. Compartmental distribution of ^{99m}Tc-ZT (I.V) and ^{99m}Tc-R7 (I.N) at different time intervals in Swiss albino mice (mean $n = 3 \pm$ S.D.).

Formulation and route of administration	Organ/tissue	Distribution of ZT in blood and brain compartments (%/g) at different time intervals (h)						
		0.25	0.5	1	2	4	6	24
^{99m}Tc-ZT/I.V. administration	Blood	10.18 ± 1.33	8.34 ± 1.16	2.21 ± 034	2.09 ± 0.20	1.83 ± 0.20	1.47 ± 0.19	0.61 ± 0.37
	Brain	0.28 ± 0.04	0.29 ± 0.03	0.07 ± 0.03	0.05 ± 0.01	0.03 ± 0.00	0.03 ± 0.02	0 ± 0.00
	Brain/blood	0.02 ± 0.00	0.03 ± 0.00	0.03 ± 0.00	0.02 ± 0.00	0.01 ± 0.00	0.01 ± 0.01	0.02 ± 0.02
^{99m}Tc-R7/I.N. administration	Blood	0.23 ± 0.09	0.22 ± 0.03	0.18 ± 0.02	0.17 ± 0.07	0.17 ± 0.05	0.15 ± 0.05	0.14 ± 0.04
	Brain	1.26 ± 0.58	1.14 ± 0.17	0.73 ± 0.12	0.59 ± 0.07	0.54 ± 0.15	0.51 ± 0.13	0.35 ± 0.07
	Brain/blood	5.39 ± 0.83	5.14 ± 1.31	3.93 ± 0.33	3.87 ± 1.98	3.26 ± 0.30	3.41 ± 0.90	2.36 ± 0.57

N.B. The mice were administered with 100 mCi ^{99m}Tc-zolmitriptan formulations and the radioactivity was measured in percent per g of tissue of the administrated dose. Each value is the mean of three estimations.

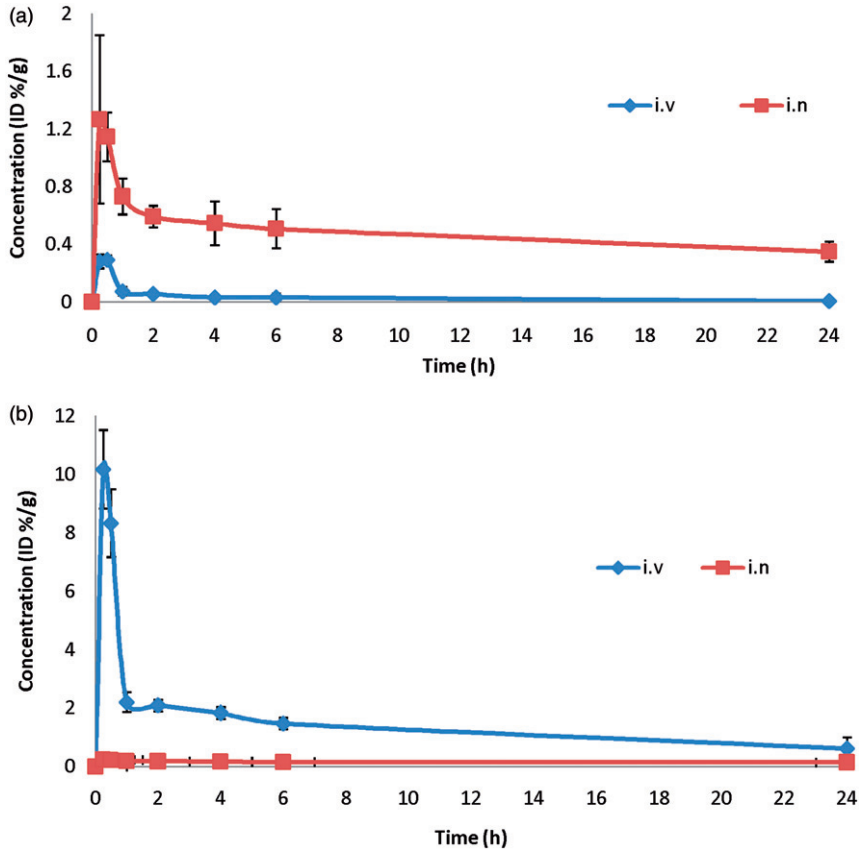

Figure 8. ZT concentration in (a) brain, (b) blood of Wister albino male mice at different time of intervals following of IV ^{99m}Tc-ZT solution in IN ^{99m}Tc-R7 novasomes, mean ± SD $n = 3$.

elucidate any possible interactions with other components. DSC thermograms of pure ZT, cholesterol, stearic acid, Span® 80 and the lyophilized optimized formulation (R7) were obtained and shown in Figure 6. The DSC scan of ZT exhibited single endothermic peak at 138.95 °C corresponding to its melting point indicating its crystalline nature. Cholesterol showed a sharp endothermic peak at 150.95 °C due to degradation and a broad endothermic peak at 37.43 °C, which may be related to loss of water molecules (Rudra et al., 2010; Al-Mahallawi et al., 2015). DSC scan of Span® 80 depicted a characteristic endothermic peak at 47.35°C. Stearic acid showed sharp endothermic peak at 65.60 °C related to its crystalline nature and a broad endothermic peak at 284.75 °C. The sharp endothermic peak of ZT was completely absent from the lyophilized optimized formulation (R7). In addition, the melting enthalpy values of stearic acid and cholesterol showed drastic depression from −564.44 and −47.70J/g to −84.99 and −5.48J/g, respectively, compared to their individual materials. This decrease in the melting enthalpy values may be associated with numerous lattice defects and the formation of amorphous regions in which the drug is embedded. These results suggest that the drug may have been homogeneously dispersed throughout the novasomes in an amorphous state.

XRD analysis

X-ray diffractograms of pure ZT, cholesterol, stearic acid, and lyophilized optimized ZT-loaded novasomes (R7) are shown in Figure 7. The diffraction pattern of pure ZT exhibited principal high intensity peaks at 2θ 20°, 22° and 30°, signifying its crystalline nature. Cholesterol showed intense

Table 4. Pharmacokinetic parameters for ZT in mice blood and brain after I.V administration ^{99m}Tc-ZT and I.N administration of the ^{99m}Tc-R7.

	I.N.		I.V.	
Pharmacokinetic parameters	Brain	Blood	Brain	Blood
$AUC_{(0–24)}$ observed (h. %/g)	11.26	3.72	0.78	34.39
$AUC_{(0–\infty)}$ (h. %/g)	23.29	16.31	0.89	45.58
$t_{1/2}$ (h)	26.05	62.31	9.46	12.61
$MRT_{(0–\infty)}$ (observed) (h)	36.38	90.45	9.35	15.75
C_{max} (%/g)	1.27	0.23	0.29	10.18
T_{max} (h)	0.50	0.25		

peaks at 2θ 15°, 16° and 18°2θ, while stearic acid showed two characteristic peaks at 2θ 20°and 25°.The diffractogram of the optimized ZT-loaded novasomes showed a disappearance of the characteristic peaks of ZT, signifying that the drug lost its crystallinity and was transformed to an amorphous state or molecular dispersion within the novasomes. The results of XRD correlated well with the results of DSC analysis, and confirmed complete amorphization of ZT within the novasomes.

In-vivo bio-distribution

Radio-labeling

A maximum radiochemical yield of $92.5 \pm 0.61\%$ was obtained at optimum labeling conditions of 2 mg ZT and 30 mg sodium dithionite. The pH of the reaction was adjusted to 6 using 0.05 M $NaHCO_3$ solution. Radio-labeling reaction was done at ambient temperature ($27 \pm 3\,^{\circ}C$) for 45 min reaction time. ^{99m}Tc-ZT complex showed good *in-vitro* stability up to 24 h (Data not shown).

Animal study

The bio-distribution study of I.V ^{99m}Tc-ZT solution and intranasal ^{99m}Tc-ZT loaded novasomes (^{99m}Tc-R7) were done on male Swiss albino mice and the radioactivity was estimated at different time intervals up to 24 h as %ID/g for different organs or body fluids (Table 3). Figure 8(a) and (b) illustrate the ZT concentrations in male Swiss albino mice blood, and brain, respectively, at different time intervals following administration of the radio-labeled formulations. Results show that ZT concentration in brain after I.N administration of the ^{99m}Tc-R7 was significantly higher than brain ZT concentration following I.V administration of ^{99m}Tc-ZT at all sampling intervals ($p < 0.05$). However, the concentration of ZT in blood after I.N administration was significantly lower than that after I.V administration ($p < 0.05$). Furthermore, the brain/blood ratios, DTP (%) were also estimated. The brain/blood ratios at all sampling intervals were significantly higher ($p < 0.05$) after I.N administration of ^{99m}Tc-R7 than I.V administrated ^{99m}Tc-ZT solution and the DTP was calculated to be 99.2%. This indicates that the prepared novasomes succeeded to penetrate the nasal membrane and deliver sufficient amount of ZT at the target site (brain) after I.N administration rather than I.V administration of ZT solution.

The pharmacokinetic parameters of both formulations (C_{max}, T_{max}, $MRT_{(0–\infty)}$, $AUC_{(0–\infty)}$ and $AUC_{(0–24)}$) were calculated by WinNonlin® and displayed in Table 4. The C_{max} in brain following I.N. administration of ^{99m}Tc-R7 and I.V administration of ^{99m}Tc-ZT were 1.27 and 0.29%/g, respectively, at same T_{max} (0.5 h). Moreover, the $AUC_{(0–\infty)}$ and $MRT_{(0–\infty)}$ in the brain after I.N administration of ^{99m}Tc-R7 were significantly higher value compared to I.V administration of ^{99m}Tc-ZT solution (23.28 and 0.89 h%/g) and (36.38 and 9.35 h), respectively ($p < 0.05$). This could be explained by the high capability of the lipid nanovesicles to permeate the nasal membrane (Salama et al., 2012; Abdelrahman et al., 2015). This suggests that the nasal route is considered as preferential route for brain targeting than I.V. route. The higher MRT value of ^{99m}Tc-R7 after I.N administration confirms the ability of the novasomes formulation to prolong and control the rate of ZT release over an extended period of time. Lipid nanovesicles have been demonstrated to have good permeability characteristics that enhance nasal penetration of many drugs through disrupting the mucosal membrane, hence increase absorption of drugs (Salama et al., 2012). Intranasal novasomes delivery enhanced ZT delivery to the brain through the olfactory pathway in which it travels from the nasal cavity to brain tissue (Illum, 2000). The small particle size helped them to squeeze themselves through the small opening in the olfactory neurons to the brain via different endocystic pathways of neuronal cells in nasal membrane (Seju et al., 2011). Similar results were obtained by Kenazawa et al., where they reported that ZT and coumarin micelle nanocarriers can be delivered to the brain due to their ability to transport trans-cellulary through olfactory membrane (Kanazawa et al., 2011).

Conclusion

Novasomes, free fatty acid enriched vesicles, were successfully prepared and loaded with a high percentage of a hydrophilic drug (ZT) in the nano-size. ^{99m}Tc-ZT-loaded novasomes showed enhanced nose to brain targeting compared with the I.V ^{99m}Tc-ZT solution. ZT-loaded novasomes administered via the nasal route may therefore constitute an advance in the management of acute migraine attacks.

Declaration of interest

The authors report no conflicts of interest. The authors alone are responsible for the content and writing of this article.

References

Abdelbary AA, AbouGhaly MH. (2015). Design and optimization of topical methotrexate loaded niosomes for enhanced management of psoriasis: application of Box-Behnken design, *in-vitro* evaluation and *in-vivo* skin deposition study. Int J Pharm 485:235–43.

Abdelbary GA, Tadros MI. (2013). Brain targeting of olanzapine via intranasal delivery of core-shell difunctional block copolymer mixed nanomicellar carriers: *in vitro* characterization, *ex vivo* estimation of nasal toxicity and *in vivo* biodistribution studies. Int J Pharm 452: 300–10.

Abdelkader H, Alani AW, Alany RG. (2014). Recent advances in non-ionic surfactant vesicles (niosomes): self-assembly, fabrication, characterization, drug delivery applications and limitations. Drug Deliv 21:87–100.

Abdelkader H, Ismail S, Kamal A, et al. (2010). Preparation of niosomes as an ocular delivery system for naltrexone hydrochloride: physicochemical characterization. Pharmazie 65:811–17.

Abdelrahman FE, Elsayed I, Gad MK, et al. (2015). Investigating the cubosomal ability for transnasal brain targeting: *in vitro* optimization, *ex vivo* permeation and *in vivo* biodistribution. Int J Pharm 490: 281–91.

Aggarwal D, Garg A, Kaur IP. (2004). Development of a topical niosomal preparation of acetazolamide: preparation and evaluation. J Pharm Pharmacol 56:1509–17.

Alhalaweh A, Andersson S, Velaga SP. (2009). Preparation of zolmitriptan-chitosan microparticles by spray drying for nasal delivery. Eur J Pharm Sci 38:206–14.

Al-Mahallawi AM, Abdelbary AA, Aburahma MH. (2015). Investigating the potential of employing bilosomes as a novel vesicular carrier for transdermal delivery of tenoxicam. Int J Pharm 485:329–40.

Anupama S, Rishabha M, Sharma PK. (2011). Novasome-A breakthrough in pharmaceutical technology a review article. Adv Biol Res 5:184–9.

Azmin MN, Florence AT, Handjani-Vila RM, et al. (1985). The effect of non-ionic surfactant vesicle (niosome) entrapment on the absorption and distribution of methotrexate in mice. J Pharm Pharmacol 37: 237–42.

Babbar AK, Singh HC, Goel UPS, et al. (2000). Evaluation of (99m)Tc-labeled photosan-3, a hematoporphyrin derivative, as a potential radiopharmaceutical for tumor scintigraphy. Nucl Med Biol 27: 587–92.

Basalious EB, Shawky N, Badr-Eldin SM. (2010). SNEDDS containing bioenhancers for improvement of dissolution and oral absorption of lacidipine. I: development and optimization. Int J Pharm 391: 203–11.

Basha M, Abdul El-Alim SH, Shamma RN, et al. (2013). Design and optimization of surfactant-based nanovesicles for ocular delivery of clotrimazole. J Liposome Res 23:203–10.

Bendas ER, Abdullah H, El-Komy MH, et al. (2013). Hydroxychloroquine niosomes: a new trend in topical management of oral lichen planus. Int J Pharm 458:287–95.

Centis V, Vermette P. (2008). Physico-chemical properties and cytotoxicity assessment of PEG-modified liposomes containing human hemoglobin. Colloids Surf B Biointerfaces 65:239–46.

Chambers MA, Wright DC, Brisker J, et al. (2004). A single dose of killed Mycobacterium bovis BCG in a novel class of adjuvant (Novasome) protects guinea pigs from lethal tuberculosis. Vaccine 22: 1063–71.

Devaraj GN, Parakh SR, Devraj R, et al. (2002). Release studies on niosomes containing fatty alcohols as bilayer stabilizers instead of cholesterol. J Colloid Interface Sci 251:360–5.

Dixon R, Warrander A. (1997). The clinical pharmacokinetics of zolmitriptan. Cephalalgia 17:15–20.

Dowson AJ, Charlesworth B. (2002). Review of zolmitriptan and its clinical applications in migraine. Expert Opin Pharmacother 3: 993–1005.

El-Laithy HM, Shoukry O, Mahran LG. (2011). Novel sugar esters proniosomes for transdermal delivery of vinpocetine: preclinical and clinical studies. Eur J Pharm Biopharm 77:43–55.

El-Setouhy DA, Basalious EB, Abdelmalak NS. (2015). Bioenhanced sublingual tablet of drug with limited permeability using novel surfactant binder and microencapsulated polysorbate: *in vitro/in vivo* evaluation. Eur J Pharm Biopharm 94:386–92.

Essa BM, Sakr TM, Khedr MA, et al. (2015). (99m)Tc-amitrole as a novel selective imaging probe for solid tumor: in silico and preclinical pharmacological study. Eur J Pharm Sci 76:102–9.

Gavini E, Rassu G, Ferraro L, et al. (2013). Influence of polymeric microcarriers on the *in vivo* intranasal uptake of an anti-migraine drug for brain targeting. Eur J Pharm Biopharm 83:174–83.

Geskovski N, Kuzmanovska S, Calis S, et al. (2013). Comparative biodistribution studies of technetium-99 m radiolabeled amphiphilic nanoparticles using three different reducing agents during the labeling procedure. J Labelled Comp Radiopharm 56:689–95.

Girotra P, Singh SK, Kumar G. (2016). Development of zolmitriptan loaded PLGA/poloxamer nanoparticles for migraine using quality by design approach. Int J Biol Macromol 85:92–101.

Glen RC, Buckingham J, Hill AP, et al. (1995). Computer-aided design and synthesis of 5-substituted tryptamines and their pharmacology at the 5-HT1D receptor: discovery of compounds with potential anti-migraine properties. J Med Chem 38:3566–80.

Gregoriadis G. (1995). Engineering liposomes for drug delivery: progress and problems. Trends Biotechnol 13:527–37.

Illum L. (2000). Transport of drugs from the nasal cavity to the central nervous system. Eur J Pharm Sci 11:1–18.

Jain R, Nabar S, Dandekar P, et al. (2010). Micellar nanocarriers: potential nose-to-brain delivery of zolmitriptan as novel migraine therapy. Pharm Res 27:655–64.

Kanazawa T, Taki H, Tanaka KO, et al. (2011). Cell-penetrating peptide-modified block copolymer micelles promote direct brain delivery via intranasal administration. Pharm Res 28:2130–9.

Kanicky JR, Shah DO. (2002). Effect of degree, type, and position of unsaturation on the pKa of long-chain fatty acids. J Colloid Interface Sci 256:201–7.

Kibbe AH, ed. (2000). Handbook of pharmaceutical excepients. 3rd edn. Washington, DC: American Pharmaceutical Association, 511–14.

Kulkarni SB, Betageri GV, Singh M. (1995). Factors affecting microencapsulation of drugs in liposomes. J Microencapsul 12: 229–46.

Lingan MA, Vijayakumar MR, Gokila A, et al. (2011). Formulation and evaluation of topical delivery system containing clobetasol propionate niosomes. Sci Revs Chem Commun 1:7–17.

Mahmoud AA, Salah S. (2012). Fast relief from migraine attacks using fast-disintegrating sublingual zolmitriptan tablets. Drug Dev Ind Pharm 38:762–9.

Manca ML, Sinico C, Octavio M, et al. (2012). Composition influence on pulmonary delivery of rifampicin liposomes. Pharmaceutics 4: 590–606.

Mittal R, Sharma A, Arora S. (2013). Ufasomes mediated cutaneous delivery of dexamethasone: formulation and evaluation of anti-inflammatory activity by Carrageenin-induced rat paw edema model. J Pharm (Cairo) 2013:680580.

Mokhtar M, Sammour OA, Hammad MA, et al. (2008). Effect of some formulation parameters on flurbiprofen encapsulation and release rates of niosomes prepared from proniosomes. Int J Pharm 361: 104–11.

Motaleb MA, El-Kolaly MT, Rashed HM, Abd El-Bary A. (2011). Novel radioiodinated sibutramine and fluoxetine as models for brain imaging. J Radioanal Nuclear Chem 289:915–21.

Motaleb MA, El-Kolaly MT, Rashed HM, Abd El-Bary A. (2012). Radioiodinated paroxetine, a novel potential radiopharmaceutical for lung perfusion scan. J Radioanal Nuclear Chem 292:629–35.

Pardakhty A, Varshosaz J, Rouholamini A. (2007). *In vitro* study of polyoxyethylene alkyl ether niosomes for delivery of insulin. Int J Pharm 328:130–41.

Pascual J. (1998). [Mechanism of action of zolmitriptan]. Neurologia 13: 9–15.

Pavelic Z, Skalko-Basnet N, Schubert R. (2001). Liposomal gels for vaginal drug delivery. Int J Pharm 219:139–49.

Prajapati ST, Patel MV, Patel CN. (2014). Preparation and evaluation of sublingual tablets of zolmitriptan. Int J Pharm Investig 4: 27–31.

Qi P, Muddukrishna SN, Torok-Both R, et al. (1996). Direct 99mTc-labeling of antibodies by sodium dithionite reduction, and role of ascorbate as a stabilizer in cysteine challenge. Nucl Med Biol 23: 827–35.

Rashed HM, Ibrahim IT, Motaleb MA, Abd El-Bary A. (2014). Preparation of radioiodinated ritodrine as a potential agent for lung imaging. J Radioanal Nuclear Chem 300:1227–33.

Rolan PE, Martin GR. (1998). Zolmitriptan: a new acute treatment for migraine. Expert Opin Investig Drugs 7:633–52.

Rudra A, Deepa RM, Ghosh MK, et al. (2010). Doxorubicin-loaded phosphatidylethanolamine-conjugated nanoliposomes: *in vitro* characterization and their accumulation in liver, kidneys, and lungs in rats. Int J Nanomedicine 5:811–23.

Salama HA, Kamel AO, Mahmoud A, et al. (2012). Brain delivery of olanzapine by intranasal administration of transfersomal vesicles. J Liposome Res 22:336–45.

Seju U, Kumar A, Sawant KK. (2011). Development and evaluation of olanzapine-loaded PLGA nanoparticles for nose-to-brain delivery: *in vitro* and *in vivo* studies. Acta Biomater 7:4169–76.

Shamma RN, Aburahma MH. (2014). Follicular delivery of spironolactone via nanostructured lipid carriers for management of alopecia. Int J Nanomedicine 9:5449–60.

Shaul Hameed Maraicar K, Narayanan T. (2014). Design and characterization of solid lipid nanoparticle by solvent evaporation method followed by homogenization. Int J Biopharmaceut 5: 190–6.

Tavano L, Vivacqua M, Carito V, et al. (2013). Doxorubicin loaded magneto-niosomes for targeted drug delivery. Colloids Surf B Biointerfaces 102:803–7.

Toshimitsu Y, Brigitte S, Florence AT. (1994). Preparation and properties of vesicles (niosomes) of sorbitan monoesters (Span 20, 40, 60 and 80) and a sorbitan triester (Span 85). Int J Pharmaceut 105:1–6.

Vyas TK, Babbar AK, Sharma RK, et al. (2005). Intranasal mucoadhesive microemulsions of zolmitriptan: preliminary studies on brain-targeting. J Drug Target 13:317–24.

Zeisig R, Shimada K, Hirota S, et al. (1996). Effect of sterical stabilization on macrophage uptake in vitro and on thickness of the fixed aqueous layer of liposomes made from alkylphosphocholines. Biochim Biophys Acta 1285:237–45.

Zhang Q, Jiang X, Lu W, et al. (2004). Preparation of nimodipine-loaded microemulsion for intranasal delivery and evaluation on the targeting efficiency to the brain. Int J Pharm 275:85–96.